# A Novel Role of the Budding Yeast Separin Esp1 in Anaphase Spindle Elongation: Evidence that Proper Spindle Association of Esp1 Is Regulated by Pds1

Sanne Jensen, Marisa Segal, Duncan J. Clarke, and Steven I. Reed

Department of Molecular Biology, The Scripps Research Institute, La Jolla, California 92037

*Abstract.* In *Saccharomyces cerevisiae*, the metaphase–anaphase transition is initiated by the anaphase-promoting complex–dependent degradation of Pds1, whereby Esp1 is activated to promote sister chromatid separation. Although this is a fundamental step in the cell cycle, little is known about the regulation of Esp1 and how loss of cohesion is coordinated with movement of the anaphase spindle. Here, we show that Esp1 has a novel role in promoting anaphase spindle elongation. The localization of Esp1 to the spindle apparatus, analyzed by live cell imaging, is regulated in a manner consistent with a function during anaphase B. The protein accumulates in the nucleus in G2 and is mobilized onto the spindle pole bodies and spindle midzone at anaphase onset, where it persists into midanaphase. Association with Pds1 occurs during S phase and is required for efficient nuclear targeting of Esp1. Spindle association is not fully restored in *pds1* mutants expressing an Esp1-nuclear localization sequence fusion protein, suggesting that Pds1 is also required to promote Esp1 spindle binding. In agreement, Pds1 interacts with the spindle at the metaphase–anaphase transition and a fraction remains at the spindle pole bodies and the spindle midzone in anaphase cells. Finally, mutational analysis reveals that the conserved COOH-terminal region of Esp1 is important for spindle interaction.

Key words:  cell cycle • Esp1/Pds1 complex • metaphase–anaphase transition • spindle elongation • budding yeast

## Introduction

Faithful chromosome segregation during cell division is of fundamental importance to the continued viability of a cell. A key event is the separation of sister chromatids at the transition from metaphase to anaphase, which in budding yeast is triggered by the ubiquitin-dependent proteolysis of the anaphase inhibitor Pds1 (Cohen-Fix et al., 1996). This event is mediated by the anaphase-promoting complex (APC),[1] which is also responsible for the destruction of other target proteins including the spindle component Ase1 and mitotic cyclins (Zachariae and Nasmyth, 1996; Juang et al., 1997). Degradation of Pds1 is necessary for the separation of sister chromatids, as mutant variants of Pds1 that cannot be degraded due to the absence of a destruction box block this process (Cohen-Fix et al., 1996).

Recently, Pds1 was revealed to form a complex with Esp1, a protein essential for viability and crucial for sister chromatid separation (Ciosk et al., 1998). *esp1^ts* mutants exhibit a failure in proper spindle behavior at the time of elongation at anaphase, and although sister chromatid separation is blocked at the restrictive temperature, cell cycle progression is not arrested in these mutants, leading to a catastrophic mitosis (McGrew et al., 1992; Ciosk et al., 1998). Esp1 is thought to be inhibited by its association with Pds1, and only when the latter is degraded is Esp1 activated to trigger proteolysis and dissociation of cohesin proteins such as Scc1 from chromosomes. This event presumably allows sister chromatids to separate when pulled by microtubules connecting their kinetochores to opposite poles of the mitotic spindle. A failure to separate sisters in the presence of a noncleavable version of Scc1 in cells with functional Esp1 protein is accompanied by a block in spindle elongation, consistent with the idea that loss of cohesion triggers anaphase (Uhlmann et al., 1999). It is not yet clear how the separation of duplicated sister chromatids (anaphase A) is coordinated with spindle elongation (anaphase B).

Recent work by Uhlmann et al. (1999) implies that Esp1 may function as a novel protease cleaving cohesin proteins,

but the exact mechanism of action and the regulation of this essential protein has not been elucidated. Functional homologues of the Esp1/Pds1 complex have been identified in *Schizosaccharomyces pombe* (Cut1/Cut2) (Uzawa et al., 1990; Funabiki et al., 1996) and Esp1-related proteins exist in *Aspergillus nidulans* (BimB) (May et al., 1992), *Xenopus*, and human (Zou et al., 1999), suggesting that control of sister chromatid separation and anaphase onset is conserved in evolutionarily diverse organisms.

In this study, we show that Esp1 activity is required past loss of cohesion at the metaphase–anaphase transition, revealing a direct role for Esp1 in spindle elongation. This is consistent with the localization of Esp1 to the spindle pole bodies (SPBs) and mitotic spindle observed in live cells and the kinetics of Esp1 spindle association. We show that Pds1 interaction is required to obtain efficient transport of Esp1 to the nucleus and for subsequent binding of the protein to the mitotic spindle, which appears to be crucial for proper anaphase progression. Furthermore, evidence is provided that an intact putative calcium-binding site in the conserved COOH-terminal region of Esp1 is important to form and maintain spindle association during anaphase.

## Materials and Methods

### Yeast Strains and Methods

The relevant genotypes of the yeast strains used in this study are listed in Table I. All strains are isogenic derivatives of BF264-15 15DU: a *ura3*Δns *ade1 his2 leu2-3,112 trp1-1[a]* (Richardson et al., 1989). Yeast media and genetic procedures were performed according to Guthrie and Fink (1991). Gene disruptions were performed by PCR-targeting technique (Wach et al., 1994).

Induction of integrated *ESP1GFP* from the *GAL1* promoter was performed as follows. Approximately $10^7$ cells of a YEPRaffinose culture was filtered onto 47-mm 0.45 μm GN-6 Metricel membrane (Gelman Sciences). Filters were placed on YEPgalactose plates for 15–30 min at room temperature. Cells were eluted into 1 M sorbitol and Esp1GFP fluorescence visualized by microscopy. For induction of Esp1GFP in time-course experiments, cells were diluted in YEPRaffinose to an $OD_{600} = 0.15$. α-factor (200 ng/ml) was added and cells were incubated at 30°C for 1 h, 2% galactose was added, and incubation was continued for 1 h. Cells were released in YEPDextrose at 30°C and samples were collected for analysis of cell-cycle progression by DAPI and protein fluorescence by microscopy.

For loss of cohesion assays, the region adjacent to the centromere of chromosome IV was visualized by using the binding of tetR-GFP fusion proteins expressed from the *CUP1* promoter (by addition of 0.25 mM $CuSO_4$ to the growth medium) to tandemly integrated tetO sequences at the *TRP1* locus (Clarke et al., 1999).

### Plasmids

ESP1-pRSG is an integrative plasmid carrying the *ESP1* open reading frame in addition to 200 bases of the 5′ flanking sequence under the control of the *GAL1* promoter. ESP1GFP-pRSG is derived from this plasmid by inserting a PCR-generated sequence encoding the GFP epitope (F64L, S65T, Q80R mutant) into a SmaI site introduced just before the stop codon. All pRSG-derived plasmids are linearized with StuI and integrants isolated by selecting for growth on dex-ura media. The parental pRSG plasmid is a derivative of pRS406 (Sikorski and Hieter, 1989), where the NaeI-PvuI fragment spanning the multiple cloning site (MCS) linker has been substituted by the NaeI-PvuI fragment from pYES2 (Invitrogen) containing a MCS and the *GAL1* promoter.

The ESP1myc18-pTRP1 plasmid was used to tag endogenous Esp1 protein with 18 myc epitopes at the COOH terminus. The integrative pTRP1 plasmid carries the sequence encoding six myc epitopes, which can be fused to a protein of interest at the NotI site (Mondesert et al., 1997). A SalI-NotI fragment spanning the last 480 bases of the *ESP1* gene was cloned into this plasmid. An additional fragment encoding 12 myc epitopes was subsequently introduced into the NotI site generating the final ESP1myc18-pTRP1 construct. The plasmid was linearized with XbaI and integrants isolated by selecting for growth on dex-trp.

The vector pOC78 (Cohen-Fix et al., 1996) was employed for tagging endogenous Pds1 internally with three hemagglutinin (HA) epitopes. To tag the Pds1-128 protein in a similar fashion, the XbaI-AvrII fragment of *pds1-128* YEp24 constituting the 3′ end of the gene with the mutation was cloned into the XbaI/AvrII sites of a pBSII-derived plasmid containing the SacI-ApaI Pds1(HA)3 fragment from pOC78. The AvrII-ApaI *pds1-128*(HA)3 fragment was used for transformation, Leu$^+$ colonies were isolated, and the presence of HA epitopes was verified by PCR.

The integrative pGAL1-Pds1Δdb plasmid described previously (Kaiser et al., 1999) was used to construct the strain expressing the nondegradable version of Pds1.

The construct expressing galactose-inducible Scc1 was generated by cloning the *SCC1* ORF into YIplac128(LEU2)GAL1 using BamHI and XhoI.

The CFP-TUB1 plasmid was constructed by replacing the GFP encoding XhoI-EcoRI fragment in pAFS91 (Straight et al., 1997) with a PCR-generated cyan fluorescent protein (CFP) fragment cut with XhoI and EcoRI. The resultant CFP-Tub1 fusion was integrated at the *URA3* locus after StuI digestion.

A panel of *esp1$^{ts}$* alleles was generated by error-prone PCR followed by in vivo gap repair as described previously (Tang and Reed, 1993). PCR mutagenesis was performed on separate *ESP1* fragments to isolate temperature-sensitive alleles mapping to the NH$_2$-terminal, central, and COOH-terminal region of Esp1. All *esp1$^{ts}$* alleles exhibited similar phenotypes. Alleles *esp1-N5* and *esp1-B3* have restrictive temperatures of 35° and 30°C, respectively. Due to the lower temperature, the *esp1-B3* mutant is more suitable for kinetic experiments.

The integrative pKGFP plasmid, which carries the *KAN$^R$* marker for G418 resistance was used to fuse the endogenous Esp1 protein to GFP. pKGFP was designed with the GFP-encoding sequence inserted after NotI, allowing in frame fusion to any protein of interest. The *ESP1* SalI-NotI fragment used to construct ESP1myc18-pTRP1 was inserted in pKGFP cut with SalI and NotI. The plasmid was linearized with XbaI and integrants were isolated by selecting for G418 resistance.

pKGFP2 was used to tag endogenous Pds1 protein at the COOH terminus. This plasmid carries a GFP sequence with additional mutations: V163A and S175G, which produces a brighter GFP fluorescent signal. To tag Pds1, a PCR-derived SalI-NotI fragment covering the last 500 bases of the *PDS1* gene was introduced into pKGFP2 at SalI-NotI. The Pds1-pKGFP2 plasmid was linearized with StuI and integrants selected by growth on G418 plates.

Plasmids ESP1(1-1568)-pRSG, ESP1(D1568A)-pRSG, and ESP1 (D1568A/D1570A)-pRSG were used to produce strains expressing the COOH-terminal truncation mutant and mutants in the putative calcium-binding site of Esp1 from the *GAL1* promoter, respectively. To generate ESP1(1-1568)-pRSG, a SalI-SmaI PCR fragment spanning the region from the internal SalI site in *ESP1* to the sequence encoding residue 1568 was introduced into the ESP1-pRSG plasmid digested with SalI and SmaI, thereby replacing the 3′ region of the *ESP1* gene. Site-directed PCR was employed to make ESP1(D1568A)-pRSG. Primers 5′ CCGAACG-GAGATTTGTCC 3′ and 5′ GCTAAATTTATCG*ATATCTTTG-GCAGTTAC-ATCCC 3′ were used to generate a mutated fragment with a single amino acid substitution (bold) and a silent mutation generating an EcoRV restriction site (underlined). This PCR product was used in a second reaction with primer 5′ GACGAGATCTTTACCCGGGTGAT-AC-GAACTTGATCGG 3′, where the SmaI site has been underlined. The cut fragment was introduced into the ESP1-pRSG vector digested with SalI and SmaI to remove the corresponding wild-type fragment. The double mutant ESP1(D1568A/D1570A)-pRSG was created by a similar PCR scheme using the following primers: 5′ CCGAACGGAGATTTGTCC3′, 5′ GCTAAATTTATCG*ATAG*CTTTGGCAGTT-ACATCCC 3′ (the modified EcoRV site is underlined and the mutation resulting in the second amino acid substitution shown in bold), and 5′GACGAGATCTTTA-CCCGGGTGATACGAACTTGATCGG 3′ (SmaI site is underlined). The cut fragment was introduced into the cut ESP1(D1568A)-pRSG vector to restore the *ESP1* gene to its full length. Clones carrying the double mutation were selected by screening for loss of the EcoRV site. GFP-tagged versions of the constructs were made by inserting a SmaI fragment encoding the GFP epitope into the respective ESP1-pRSG plasmids opened by SmaI.

The integrative plasmid ESP1GFPNLS-pRSG was used to make strains expressing Esp1GFP fused at the COOH terminus to the SV40 NLS from the *GAL1* promoter. A PCR fragment produced with following primers: 5′ CTAGCCCGGGAAGAAAAAGCGAAAGGTCG-GCCGCATGAG-TAAAG 3′ and 5′ GCTACCCGGGGACCTTTCGCTTCTTCTTGGG-TTTGTATAGTTCATCCATGC 3′, where SmaI sites are underlined and the SV40 NLS sequence is shown in bold, was inserted into the ESP1-pRSG plasmid digested with SmaI.

Plasmid ESP1-pRS415 was made by inserting the *ESP1* promoter sequence and ORF into the ARS/CEN plasmid pRS415 digested with SalI

*Table I. Yeast Strains Used in this Study*

| Strain | Relevant genotype |
| --- | --- |
| SY101 | *MATa bar1 GAL1:ESP1:GFP (URA3)* |
| SY102 | *MATa pds1::KAN^R GAL1:ESP1:GFP (URA3)* |
| SY103 | *MATa pds1-128 GAL1:ESP1:GFP (URA3)* |
| SY104 | *MATa GAL1:ESP1:GFP (URA3)* |
| SY105 | *MATa GAL1:ESP1:GFP:NLS (URA3)* |
| SY106 | *MATa pds1::KAN^R GAL1:ESP1:GFP:NLS (URA3)* |
| SY107 | *MATa pds1-128 GAL1:ESP1:GFP:NLS (URA3)* |
| SY108 | *MATa bar1 pep4::URA3 ESP1::ESP1(MYC)18(TRP1)* |
| SY109 | *MATa bar1 pep4::URA3 ESP1::ESP1(MYC)18(TRP1) PDS1::PDS1(HA)3(LEU2)* |
| SY110 | *MATa bar1 pep4::URA3 ESP1::ESP1(MYC)18(TRP1) pds1-128::pds1-128(HA)3(LEU2)* |
| SY111 | *MATa bar1 PDS1::PDS1(HA)3(LEU2)* |
| SY112 | *MATa PDS1::PDS1(HA)3(LEU2) GAL1:ESP1:GFP(URA3)* |
| SY113 | *MATa PDS1::PDS1(HA)3(LEU2) GAL1:ESP1(1-1568):GFP(URA3)* |
| SY114 | *MATa PDS1::PDS1(HA)3(LEU2) GAL1:ESP1(D1568A):GFP(URA3)* |
| SY115 | *MATa PDS1::PDS1(HA)3(LEU2) GAL1:ESP1(D1568A/D1570A):GFP(URA3)* |
| SY116 | *MATa bar1 PDS1::PDS1:GFP (KAN^R)* |
| SY117 | *MATα esp1::KAN^R trp1::esp1-N5:TRP1* |
| SY118 | *MATa bar1 scc1::KAN^R GAL1:SCC1 (LEU2) ura3::HIS3:CFP-TUB1 (URA3) CUP1:GFP:tetR(KAN^R) trp1::TRP1-(tetO)* |
| SY119 | *MATa bar1 esp1::KAN^R esp1-B3 (TRP1) ura3::HIS3:CFP-TUB1 (URA3) CUP1:GFP:tetR(KAN^R) trp1::TRP1-(tetO)* |
| SY120 | *MATa bar1 esp1::KAN^R esp1-B3 (TRP1) scc1::KAN^R GAL1:SCC1 (LEU2) ura3::HIS3:CFP-TUB1 (URA3) CUP1:GFP:tetR(KAN^R) trp1::TRP1-(tetO)* |
| SY121 | *MATa GAL1:ESP1:GFP (URA3) PDS1Δdb (LEU2)* |
| SY122 | *MATa esp1::KAN^R esp1-N5 (TRP1)* |
| SY201 | *MATa/α ESP1::ESP1:GFP(KAN^R)/ESP1::ESP1:GFP(KAN^R)* |
| SY202 | *MATa/α PDS1::PDS1:GFP(KAN^R)* |
| SY203 | *MATa/α GAL1:ESP1:GFP (URA3)/ura3* |
| SY204 | *MATa/α ase1::KAN^R/ase1::KAN^R GAL1:ESP1:GFP (URA3)/ura3* |
| SY205 | *MATa/α GAL1:ESP1:GFP (URA3)/ura3 SPC29:CFP (KAN^R)* |
| SY206 | *MATa/α GAL1:ESP1:GFP (URA3)/ura3::HIS3:CFP-TUB1 (URA3)* |
| SY207 | *MATa/α PDS1::PDS1:GFP (KAN^R)/SPC29:CFP (KAN^R)* |
| SY208 | *MATa/α PDS1::PDS1:GFP (KAN^R) ura3::HIS3:CFP-TUB1 (URA3)/ura3* |

and SacI (Sikorski and Hieter, 1989). To generate ESP1(1-1568)-pRS415, the SpeI fragment from ESP1(1-1568)-pRSG containing the 3′ end of the *ESP1* gene was introduced into the ESP1-pRS415 plasmid cut with SpeI. The *ESP1* calcium-binding site mutants were cloned into pRS415 by substituting the NdeI fragment derived from ESP1(D1568A)- and ESP1(D1568A/D1570A)-pRSG with the corresponding fragment in ESP1-pRS415. All plasmids were subjected to sequencing to verify their integrity.

## Cell Biology Protocols

Fluorescence and differential interference contrast (DIC) microscopy was performed using an Eclipse E800 microscope (Nikon) with a 100× objective. Cell images were captured with a Quantix CCD (Photometrics) camera using IPlab Spectrum software (Signal Analytics Co.). Spindle measurements were performed on captured images using the NIH Image measuring tool calibrated with a stage micrometer. For microscopy of live cells expressing either wild-type/mutant Esp1GFP or Pds1GFP, cells were grown in YEPRaffinose/YEPGalactose or YEPDextrose, respectively, containing extra supplement of adenine (0.2 mg/ml). Images were acquired using 500-ms exposures. For simultaneous detection of GFP- and CFP-labeled proteins, images were captured using a Photometrics CH350L CCD camera on an Olympus IX70 inverted microscope with a 100× magnification. Images were taken of a single focal plane and later manipulated using SoftWoRx software (Applied Precision Inc.). Cross bleeding of GFP and CFP signals did not occur as there was no CFP signal in the GFP channel and vice-versa in singly tagged strains. Nuclei were visualized with DAPI as described previously (Mondesert et al., 1997).

Cell cultures were analyzed for DNA content using flow cytometry as described previously (Mondesert et al., 1997).

## Immunoprecipitation and Immunostaining

Protein isolation was essentially as previously described (Kaiser et al., 1999). Cells were broken by glass beads in NP-40 buffer (50 mM Tris-HCl,

pH 7.5, 150 mM NaCl, 0.1% NP-40, 10 mM sodium pyrophosphate, 5 mM EDTA, 5 mM EGTA, 0.1 mM orthovanadate, 1 mM PMSF, 2 mg/ml aprotinin, leupeptin, and pepstatin A). A total of 750 μg of extract was incubated with myc9E10 antibody prebound to protein A sepharose or with 12CA5 antibody cross linked to protein A sepharose for 2 h, and immunocomplexes were washed four times with 1 ml of extraction buffer. Bound proteins were eluted by boiling in 2× SDS sample buffer, separated by SDS-PAGE (7.5% protein gels), and analyzed by immunostaining with anti–HA antibody (12CA5, BabCO), anti–myc antibody (9E10) and anti–GFP antibody (CLONTECH Laboratories, Inc.). Extracts prepared solely for immunostaining were separated on 8.5% SDS-polyacrylamide gels. Cdc28 protein serving as a loading control was recognized by the anti–PSTAIRE antibody.

## Results

### Cell Cycle–dependent Distribution of Esp1 in Live Yeast Cells

To gain insight into the regulation and function of Esp1 in *S. cerevisiae*, we initiated a study of the localization of this protein in live cells. Unlike Pds1, the level of Esp1 is not highly regulated in the cell cycle. The abundance of Esp1 protein was examined in synchronized cells expressing endogenous Esp1 fused to 18 myc epitopes at its COOH-terminus after release from an α-factor–induced G1 block (Fig. 1 A). The level of this fully functional fusion protein is approximately threefold lower in G1 than in the rest of the cell cycle, where it appears to be constant. The synchrony of the cells was verified by flow cytometry (data not shown).

To monitor if the localization profile of Esp1 in living cells changes through the cell cycle, a gene encoding Esp1 tagged with the green fluorescent protein (GFP) was integrated into a wild-type strain. This fusion protein complements an *esp1^ts* mutation, and cells overexpressing Esp1GFP under the control of the *GAL1* promoter grow normally (not shown). The strain was arrested in G1 using α-factor and Esp1GFP protein induced transiently by addition of galactose 30 min before release from the arrest into glucose-containing medium. At given intervals, the localization of Esp1GFP was monitored in live cells by microscopy and the cell-cycle distribution followed by DAPI staining (Fig. 1 B). The fluorescent signal of Esp1GFP was delocalized throughout the entire cell in unbudded cells (G1). In G2, the protein was concentrated in the nucleus, and shortly thereafter was mobilized to the SPBs and the metaphase spindle (but see below). As cells progressed into anaphase, Esp1 signal was observed almost exclusively at the 2-μm region of the spindle midzone in addition to the SPBs. The localization of Esp1GFP at different stages of the cell cycle is illustrated in Fig. 2 A, where the protein was induced to ~10-fold higher levels compared with endogenous level (not shown). The distribution of Esp1 observed under these circumstances is not a result of overexpression, as the same localization pattern is observed in a strain expressing Esp1GFP from the endogenous promoter (Fig. 2 A, i). The association of Esp1 with SPBs and spindle was confirmed in colocalization experiments with strains expressing galactose-inducible Esp1GFP and endogenous levels of the SPB marker Spc29 fused to CFP (Spc29CFP) or a CFP-tagged version of tubulin (CFPTub1), respectively (Fig. 2 B). The length of the spindles labeled by Esp1GFP exhibited a broad distribution (Fig. 2 C). Relatively few Esp1-decorated spindles were measured as 2 μm and shorter, and in all cases the spindles were already oriented along the mother-bud axis. This is in contrast with tubulin staining of an analogous population, where 2-μm metaphase spindles are the most frequently observed class, and anaphase spindles of intermediate length are quite rare (data not shown). These data indicate that Esp1 labels the spindle at the metaphase–anaphase transition and not in G2 or during the bulk of metaphase. The majority of Esp1GFP anaphase spindles fell into the 3–6-μm intermediate range, but even spindles up to 9 μm were observed, although fully extended anaphase spindles of 10–12 μm did not contain Esp1. The appearance of Esp1 on spindles at the metaphase–anaphase transition, its persistence on anaphase spindles, and the specific enrichment of Esp1 at the spindle midzone, a structure important for anaphase spindle elongation in yeast (Pellman et al., 1995) is suggestive of a role of Esp1 in spindle elongation at anaphase.

### Esp1 Is Required for Anaphase Spindle Movement

We next asked whether Esp1 indeed plays a direct role in spindle elongation. For this purpose, mutants deleted for the cohesin *SCC1* were employed to circumvent the obstacle of Esp1 being required for the earlier event in loss of cohesion. In *scc1* mutants, cohesion is defective and sister chromatid separation occurs prematurely (Michaelis et al., 1997). *scc1Δ*, *esp1^ts^scc1Δ* (kept alive with galactose-induced Scc1), and *esp1^ts* mutant cells were synchronized in G1 with
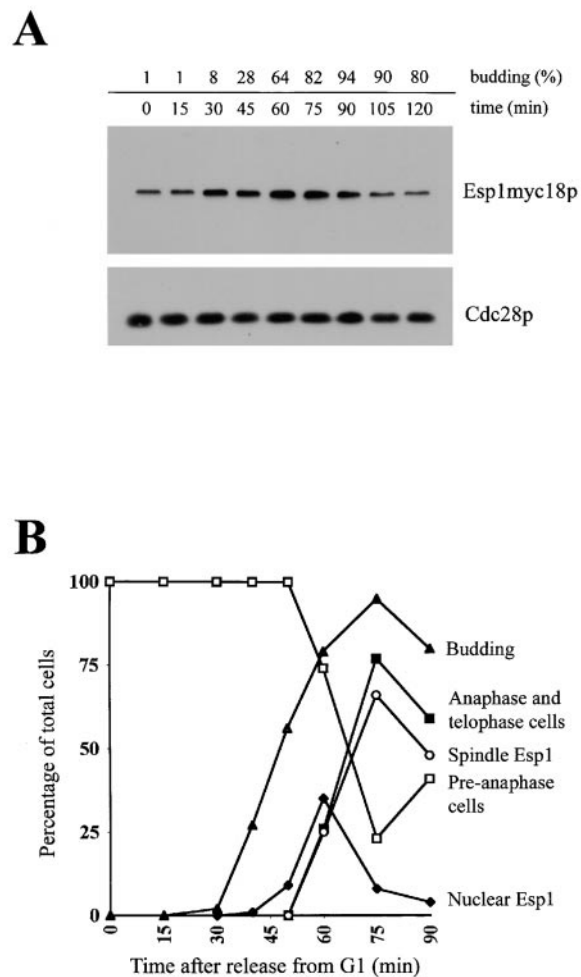




*Figure 1.* Cell cycle–dependent regulation of Esp1. (A) Esp1 protein level during the cell cycle. Strain carrying epitope-tagged Esp1 integrated at the chromosomal locus (SY108) was arrested in G1 with α-factor. Cells were released into YEPDextrose at 25°C and aliquots removed at indicated times for analysis of cell morphology, Esp1 and Cdc28 protein levels, and FACS® analysis. (B) Cell cycle changes in Esp1 localization in live cells. Strain carrying *GAL1*-inducible *ESP1GFP* (SY101) was arrested in G1 with α-factor. 30 min before release, 2% galactose was added to induce Esp1GFP. Cells were released into YEPDextrose at 30°C, and aliquots were removed at intervals for analysis by real time microscopy, determination of budding index and cell-cycle progression by DAPI stain. (□) Cells with preanaphase nuclear morphology; (■) cells with anaphase and telophase nuclear morphology; (▲) budding index; (◆) nuclear localization of Esp1; (○) spindle localization of Esp1.

α-factor and released into YEPDextrose at the restrictive temperature of the *esp1^ts* mutation. Wild-type cells were included for reference. The timing of budding, loss of cohesion (visualized using a GFP marker on chromosome IV; Clarke et al., 1999), and spindle morphology (visualized by CFP-labeled tubulin) were analyzed as the cells progressed through the cell cycle (Fig. 3). All strains budded and assembled bipolar spindles with similar kinetics. Whereas *scc1Δ* cells separated sister chromatids prematurely and were capable of elongating their spindles (Fig. 3 B), *esp1^ts* cells, as originally reported, failed to separate sister chromatids and maintained short spindles until the cells exited
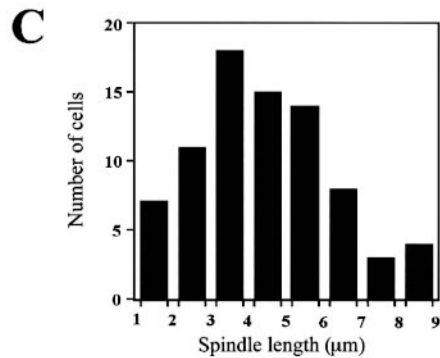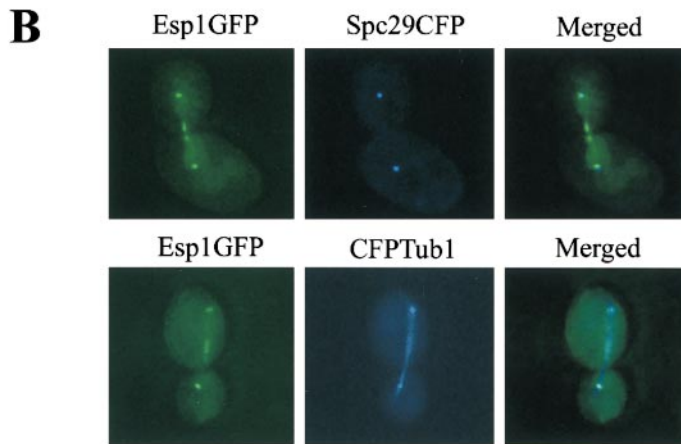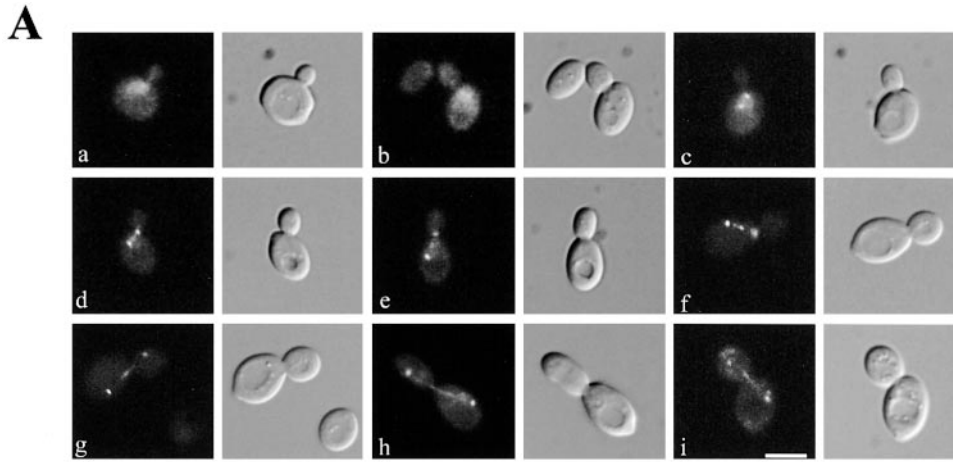
**A**



**B**

Esp1GFP    Spc29CFP    Merged

Esp1GFP    CFPTub1    Merged



**C**



*Figure 2.* Localization of Esp1GFP at different stages of the cell cycle. (A) Diploid cells carrying an integrated *ESP1GFP* allele (SY203) grown in YEPRaffinose were collected on a nitrocellulose filter and induced 15 min on a YEPGalactose plate. Cells were examined by microscopy and images acquired of GFP signal and DIC. (a and b) Nuclear Esp1GFP signal in late G2 cells; (c) metaphase spindle and SPB stain of Esp1; (d–h) anaphase spindles stained by Esp1; (i) anaphase spindle stain in cells expressing Esp1GFP from the native promoter (SY201). Scale bar: 10 μm. (B) Images of cells expressing Esp1GFP and either Spc29CFP (SY205, top) or CFPTub1 (SY206, bottom) captured and merged as described in Materials and Methods. (C) The length distribution of spindles labeled by Esp1GFP. Spindles measured on cells treated as described in A.

mitosis (Fig. 3 C). If Esp1 activity is solely required to promote loss of cohesion, one would predict that an *esp1^{ts}scc1*Δ double mutant would elongate spindles similarly to the *scc1*Δ mutant. However, there were virtually no elongated spindles observed in the *esp1^{ts}scc1*Δ mutant in the absence of cohesion and, as in the case of the *esp1^{ts}* cells, the short spindles were maintained for the time it took the *scc1*Δ mutant to proceed through anaphase (Fig. 3 D). These data unequivocally show that Esp1 is required for spindle elongation during anaphase, and not merely to promote loss of cohesion at the metaphase-to-anaphase transition. Consistent with the role of Esp1 in activation of spindle elongation, *ndc10-1* cells, which elongate spindles in the absence of chromosome segregation due to defective kinetochores (Goh and Kilmartin, 1993), fail to elongate spindles in the absence of Esp1 activity (data not shown).

### Association with Pds1 Is Essential for Proper Esp1 Localization

As an initial attempt to understand how this novel function of Esp1 might be regulated, we set out to investigate how Esp1 spindle localization is controlled. Given the accumulation of Esp1 protein at the midzone, we examined the possible connection between this association and a known component of the spindle midzone in yeast, Ase1. Although this protein is important for efficient anaphase spindle elongation, it is not essential, and *ase1* mutants are able to faithfully segregate chromosomes despite their unstable spindles (Pellman et al., 1995; Juang et al., 1997). The *ESP1GFP* gene was integrated into an *ase1*Δ mutant and the protein visualized after transient induction, as described above. The localization of Esp1 to the nucleus and the SPBs was not affected in this mutant; however, no sig-
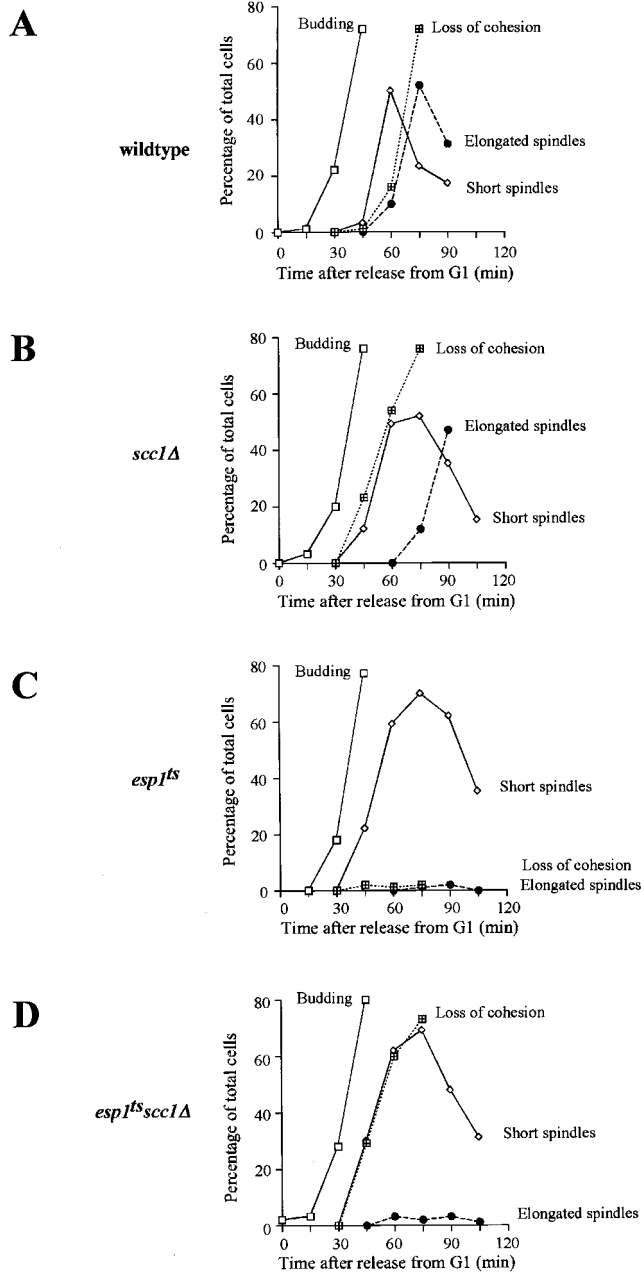
**A**



**B**



**C**



**D**



*Figure 3.* Esp1 is essential for spindle elongation. Cells of wild-type (A), *scc1*Δ (SY118) (B), *esp1-B3* (SY119) (C), and *scc1*Δ*esp1-B3* (SY120) (D) strains containing CFP-tubulin and GFP-labeled centromeres were synchronized in G1 in YEPDextrose by addition of α-factor, and subsequently released into YEPDextrose at 31.5°C. Aliquots were removed at 15-min intervals for scoring budding index, spindle morphology, and loss of cohesion for chromosome IV. Short spindles (<2.5 μm) and elongated spindles (>4 μm) were scored by measurement of digital images. More than 200 cells were counted for each time point.

nal at the spindle midzone was observed in >500 cells analyzed (Fig. 4 A). There are two possible explanations for this result. Either Ase1 interaction is required to mediate midzone binding of Esp1 or the structure of the midzone in *ase1* mutants is perturbed, hampering Esp1 association or detection. Coimmunoprecipitation experiments on a

strain with epitope-tagged versions of Esp1 and Ase1 expressed from their chromosomal loci revealed no interaction between the two components under a variety of test conditions (not shown). It is therefore more likely that the absence of Esp1 at the midzone in *ase1* mutants is due to structural alterations of the midzone. Deletion of *ASE1* in an *esp1^{ts}* mutant exacerbates the temperature sensitivity of the strain, consistent with the idea that the spindle midzone is important for Esp1 function (data not shown).

The only protein identified to date that interacts with Esp1 is the anaphase inhibitor Pds1. To examine what effect Esp1/Pds1 complex formation has on the subcellular distribution of Esp1, the Esp1GFP protein was expressed and followed in a *pds1*Δ mutant at the permissive temperature. Surprisingly, the fluorescent signal was delocalized within the whole cell throughout the entire cell cycle. There was no detectable accumulation of Esp1GFP in the nucleus or spindle association (Fig. 4 B). Although the *pds1*Δ strain is viable, the mutant grows poorly and the cells die at 28°C in the genetic background used for these studies. We therefore examined the localization of Esp1 in the less severe *pds1-128^{ts}* mutant, which has a restrictive temperature of 37°C. Esp1GFP exhibited a similar localization profile in this mutant at the permissive temperature to that observed in the *pds1*Δ strain (Fig. 4 C). Indirect immunofluorescence on cells expressing endogenous myc18-tagged Esp1 further confirmed the requirement of a functional Pds1 for correct localization of Esp1, as *pds1-128* cells failed to show nuclear or spindle staining of Esp1 (data not shown).

By two-hybrid analysis we found that the NH$_2$-terminal domain of Esp1 spanning residues 1–535 interacts with the COOH-terminal region (residues 300–373) of Pds1 (not shown). Since the *pds1-128^{ts}* mutation affects the extreme COOH terminus of Pds1 (D.J. Clarke and S.I. Reed, unpublished data), it is possible that the mutant Pds1 protein is incapable of interacting with Esp1. To test this directly, immunoprecipitation was performed on extract from strains encoding endogenous myc18-tagged Esp1 and wild-type Pds1 or Pds1-128 protein tagged with three copies of the HA epitope. The level of coprecipitated Pds1-128 protein was significantly lower than the amount of Pds1 present in the immunoprecipitated wild-type sample (Fig. 4 D). The reduction in Esp1/Pds1 complex formation in the *pds1-128* strain, however, is not due to an inability of the mutant Pds1 protein to interact with Esp1, as revealed by two-hybrid analysis (not shown), but rather reflects the high instability and low steady state level of the Pds1-128 protein. Thus, we conclude that complex formation between Esp1 and Pds1 is required to ensure proper movement of Esp1 to the nucleus and spindle, where it can exert its anaphase functions.

### Pds1 Transports Esp1 into the Nucleus and Promotes Spindle Association

To address whether the lack of Esp1 spindle association in strains compromised for Pds1 function could simply reflect the absence of nuclear accumulation of Esp1, we investigated the effect of fusing a nuclear localization sequence (NLS) to Esp1 on its localization. For this purpose, a peptide encoding the potent SV40 NLS (KKKRKV) was
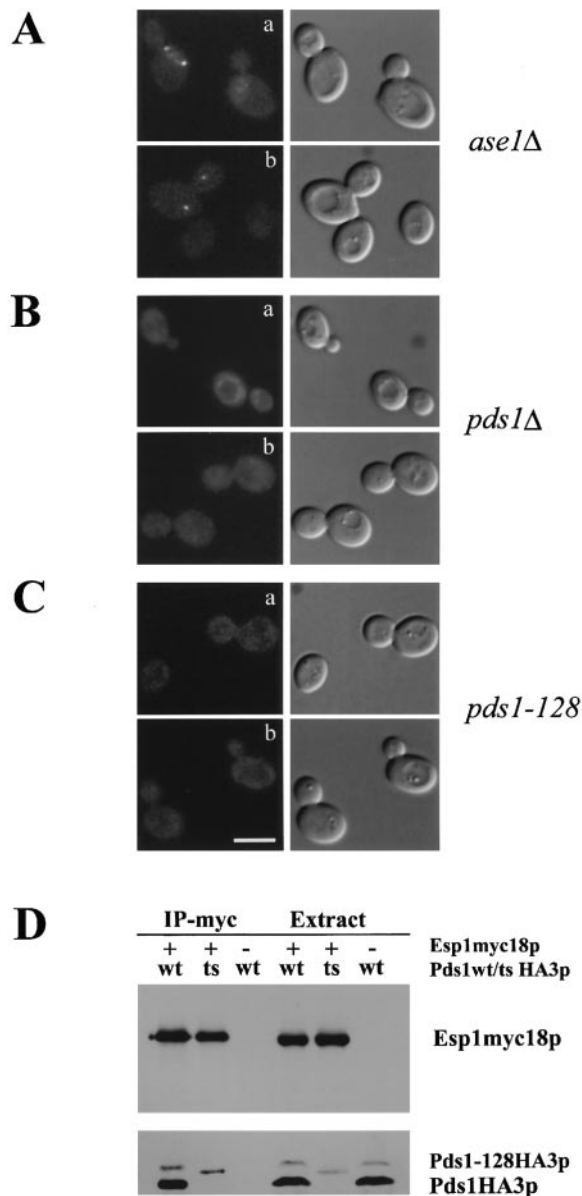
A
a
b
ase1Δ

B
a
b
pds1Δ

C
a
b
pds1-128

D

| IP-myc | | | Extract | | | |
|---|---|---|---|---|---|---|
| + | + | - | + | + | - | Esp1myc18p |
| wt | ts | wt | wt | ts | wt | Pds1wt/ts HA3p |

Esp1myc18p

Pds1-128HA3p
Pds1HA3p

*Figure 4.* Proper Esp1 localization depends on Pds1. (A, a and b) Esp1 signal at the spindle midzone is absent in *ase1Δ* mutant. A diploid *ase1Δ* strain carrying *GAL1*-inducible *ESP1*GFP (SY204) was examined by microscopy after induction, as described in Fig. 2. (B, a and b) Localization of Esp1 in *pds1Δ* mutant. Haploid *pds1Δ* cells expressing Esp1GFP from the *GAL1* promoter (SY102) were treated as in A. (C, a and b) Movement of Esp1 to nucleus and spindle is reduced in a *pds1-128* mutant. Haploid *pds1-128* cells with *ESP1*GFP integrated (SY103) were analyzed as above. (D) Comparison of Esp1/Pds1 complex formation in exponentially growing wild-type cells and *pds1-128* cells. Strains carrying endogenous myc18-tagged Esp1 and HA3-tagged Pds1 (wt) (SY109) or Pds1-128 (ts) (SY110) were grown at 25°C. Extracts were immunoprecipitated with anti–myc antibody. Samples were analyzed by SDS-PAGE followed by immunostaining with anti–myc antibody and anti–HA antibody. An isogenic control strain expressing endogenous Pds1HA3 protein was included to show specificity of the anti–myc antibody (SY111). Note that the additional amino acids at the COOH terminus of the Pds1-128 protein causes it to migrate at a slightly lower mobility.

fused to the COOH terminus of the Esp1GFP protein. This chimeric protein retains the ability to complement an *esp1ts* mutation when overexpressed from the *GAL1* promoter (not shown). In wild-type cells, the Esp1GFPNLS protein exhibited a localization profile similar to that of Esp1 fused to GFP alone (Fig. 5 A, top). In contrast, expression of Esp1GFPNLS in the *pds1-128* mutant now resulted in accumulation of the protein in the nucleus and subsequent labeling of the SPBs and weak spindle association. However, increasing the nuclear import of Esp1 in *pds1-128* cells was not sufficient to achieve a strong spindle fluorescence, as seen in wild-type cells (Fig. 5 A, middle), suggesting that Pds1 association may also be required to obtain efficient Esp1 spindle interaction. This is consistent with the observation that there is no detectable spindle fluorescence in *pds1Δ* cells expressing Esp1GFPNLS (data not shown). Esp1 did label the SPBs in this mutant, demonstrating that Esp1 has the ability to bind the SPBs in the absence of Pds1 (Fig. 5 A, bottom). This is perhaps not surprising as mutants deleted for *PDS1* are viable at low temperatures and unless the essential function of Esp1 is independent of its spindle localization, Esp1 must have intrinsic spindle binding activity sufficient for viability. This association, however, is clearly more efficient when Pds1 is present. Expressing the Esp1GFPNLS version in a *pds1Δ* mutant leads to partial suppression of the temperature-sensitive phenotype at 30°C, whereas the *pds1Δ* mutant expressing Esp1GFP is dead at this temperature (not shown). This further supports the notion that an important function of Pds1 is to target Esp1 to the nucleus and subsequently to the spindle.

Surprisingly, the timing of nuclear concentration of Esp1GFPNLS in wild-type cells is unaltered compared with that of Esp1 fused to GFP alone. Both proteins accumulate in the nucleus in G2. This suggests that additional mechanisms regulate nuclear translocation of Esp1 (see Discussion).

To further confirm that association with Pds1 directs Esp1 localization, we constructed a strain expressing Esp1GFP and a nondegradable version of Pds1 (Pds1Δdb) from the *GAL1* promoter. Induction of Pds1Δdb protein led to a strong nuclear accumulation of Esp1GFP in unbudded cells, which was never observed in unbudded control cells, where the level of endogenous Pds1 is low due to active Pds1 proteolysis early in the cell cycle (Fig. 5 B). Of >300 unbudded cells counted, ~65% showed a strong Esp1 signal always colocalizing with the DAPI signal. This number is probably a low estimate as fixation often reduced the intensity of the Esp1GFP signal. Thus, expressing Pds1 prematurely in the cell cycle promotes early translocation of Esp1 to the nucleus.

### Pds1 Localizes to the Spindle Apparatus in Budding Yeast

Given the observation that Esp1 localization is controlled by Pds1, one would expect the two components to display similarities in their distribution at times of the cell cycle when Esp1 localization is changing. To investigate this, a strain was constructed expressing endogenous Pds1 fused at its COOH terminus to GFP, which is fully functional and regulated during the cell cycle with similar kinetics as
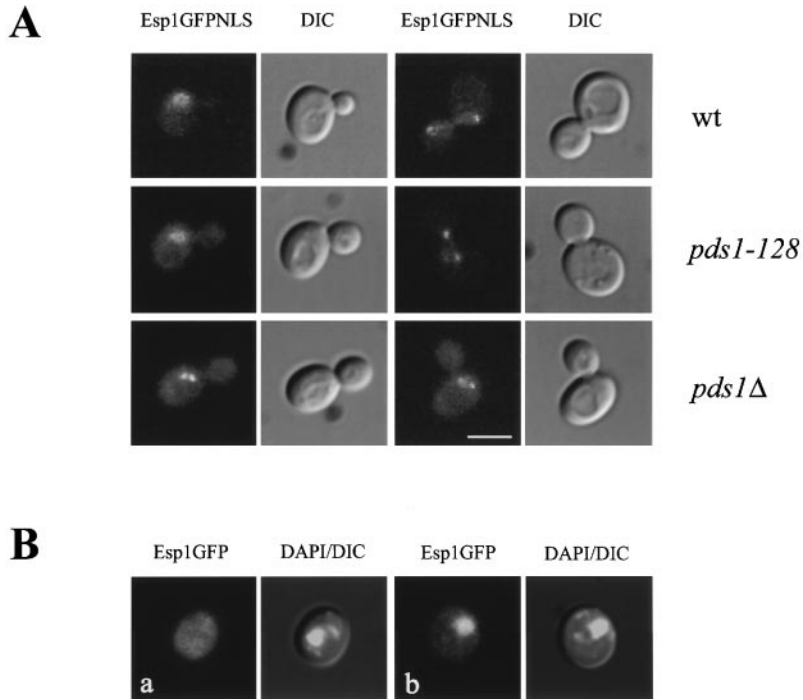
*Figure 5.* Pds1 is required to load Esp1 onto the spindle. (A) A version of Esp1GFP fused at its COOH terminus to the SV40 NLS was integrated into a wild-type strain (SY105, top), a *pds1-128* mutant (SY107, middle), and a *pds1Δ* mutant (SY106, bottom). The Esp1GFPNLS protein was induced for 20 min from the *GAL1* promoter on solid YEPGalactose medium. (Left) GFP fluorescence; (right) DIC. Scale bar: 10 μm. (B) Expression of a nondestructable Pds1 (Pds1Δdb) leads to premature nuclear localization of Esp1. A strain carrying *GAL1*-inducible integrated *ESP1*GFP and *PDS1*Δdb alleles (SY121) (b) was grown in YEPRaffinose. After 1-h galactose induction at 30°C, cells were fixed 30 min in 3.75% formaldehyde and stained with DAPI to visualize nuclei. (Left) Esp1GFP fluorescence; (right) DAPI/DIC overlay. A control strain carrying only a *GAL1*-inducible *ESP1*GFP allele (SY104) was analyzed in a similar fashion (a).

the wild-type protein (data not shown). Cells were synchronized with α-factor and, after release from G1, the localization of Pds1GFP was monitored by fluorescence microscopy. Nuclear morphology scored by DAPI and bud development were used as markers for cell-cycle progression (Fig. 6 A). Cells in G1 contained no Pds1GFP fluorescence, as expected, since Pds1 protein first appears after bud emergence. As cells progressed through S-phase, Pds1GFP protein accumulated almost exclusively in the nucleus. The nuclear localization of Pds1 has been shown in an earlier study by indirect immunofluorescence (Alexandru et al., 1999), where Pds1myc18 protein was shown to localize in the nucleus concomitant with bud emergence. In our study, there is a temporal lag between bud emergence and nuclear signal of Pds1 (~10–15 min), which may reflect the relatively weaker signal obtained with a single GFP tag. At the metaphase-to-anaphase transition, the majority of Pds1GFP disappeared, but, surprisingly, a fraction remained nuclear and often associated with the spindle apparatus. There was a strong fluorescent signal of Pds1 at the SPBs and a 2-μm bar at the spindle midzone in anaphase cells (Fig. 6 B). To confirm that the Pds1GFP spots indeed colocalize with SPBs, a strain was constructed expressing Pds1GFP and Spc29CFP, and fluorescence images captured on live cells (Fig. 6 C, top). The spindle association of Pds1 was also verified by simultaneous labeling of Pds1GFP and CFP-fused tubulin (Fig. 6 C, bottom). The length distribution of spindles labeled by Pds1 was less broad than that observed with Esp1 (Figs. 6 D and 2 D). Most spindles were within the 2–4-μm range, but anaphase spindles stained by Pds1 were seen up to 7-μm long. According to live cell measurements in haploid cells, a yeast spindle is between 2.5- and 3-μm long when chromosome separation begins (Straight et al., 1997). The association of Pds1 with mitotic spindles is consistent with the idea that Pds1 promotes Esp1 spindle binding by actually loading Esp1 onto the spindle apparatus at metaphase–anaphase transition. Furthermore, the bias to-

ward shorter spindles stained with Pds1, as compared with Esp1, suggests that Esp1 can be retained on the spindle once Pds1 is removed or degraded. Finally, the localization of Pds1 to the spindle is not altered in an *esp1ts* mutant, suggesting that Esp1 is not required for this process (data not shown).

## Complex Formation between Esp1 and Pds1 Is Established Early in the Cell Cycle

To establish when in the cell cycle the complex between Esp1 and Pds1 is formed, cells expressing endogenous myc18-tagged Esp1 and HA3-tagged Pds1 were arrested in G1 by α-factor. The cells were released at 22°C to slow down the cell cycle, providing a broader temporal window in which to monitor the timing of Esp1/Pds1 complex formation. After release, samples were collected at intervals for immunoprecipitation, immunoblotting, and FACS® analysis to confirm the synchrony. As is evident, the Esp1/Pds1 complex is formed at the time Pds1 first appears in the cell cycle and persists until anaphase, where Pds1 degradation is initiated (Fig. 7, A and B). Therefore, Esp1 activity is likely to be controlled by Pds1 through most of the cell cycle. A reconstitution experiment, where extract containing Esp1myc18 protein was mixed with extract containing Pds1HA3 protein followed by immunoprecipitation, showed that a complex between the two components could not be formed under these in vitro conditions (Fig. 7 C). This confirms that the Esp1/Pds1 association shown in Fig. 7 B reflects the true in vivo situation and is not an artifact of extraction. The coprecipitation result also correlates with the similar localization profile of the Esp1 and Pds1 proteins.

## A Putative Calcium Binding Site in the COOH-Terminal Domain of Esp1 Is Important for Spindle Binding

Esp1 is a large protein composed of a total of 1,630 amino acid residues (McGrew et al., 1992). Little information can
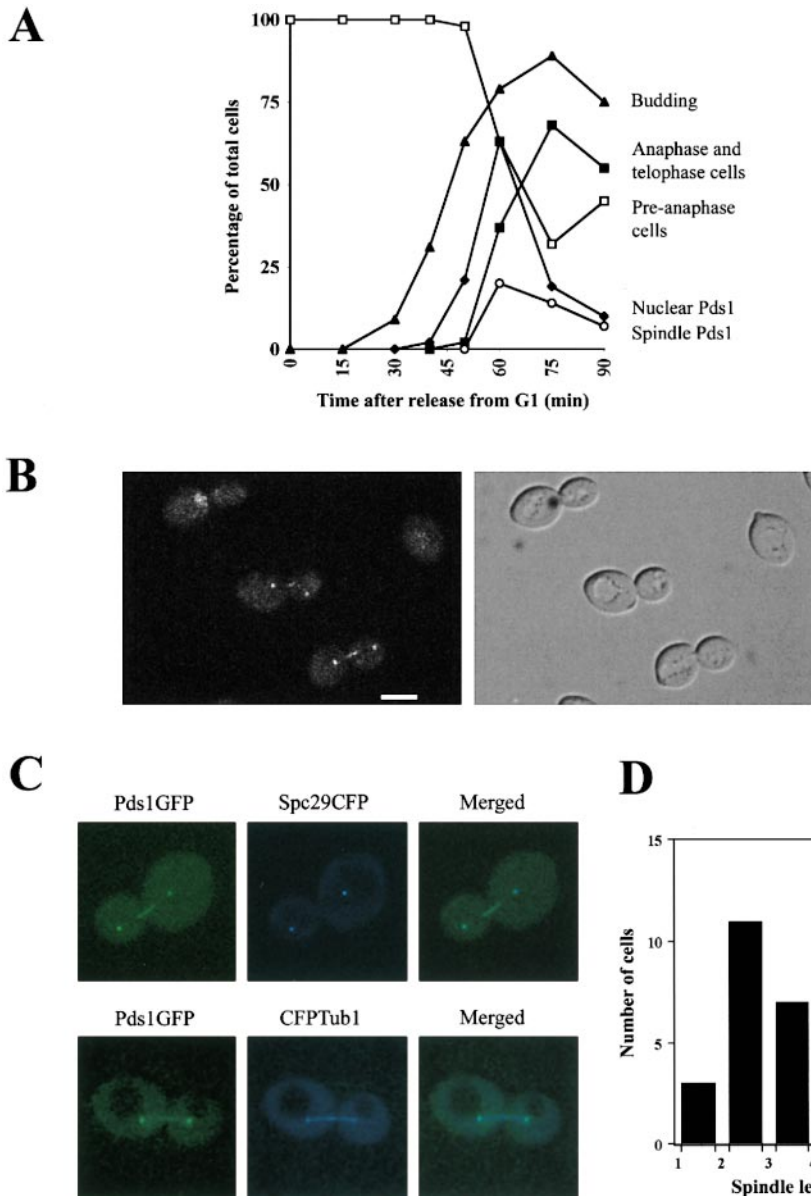
**A**



**B**



**C**



**D**



*Figure 6.* Pds1 associates with the mitotic spindle apparatus. (A) A strain carrying *PDS1* fused at the COOH-terminal end to GFP integrated at the chromosomal locus (SY116) was arrested in G1 with α-factor. After release into YEP-Dextrose at 30°C, aliquots were taken for scoring budding index, cell-cycle progression by DAPI, and real-time localization of Pds1GFP. (□) Cells with pre-anaphase nuclear morphology; (■) cells with anaphase and telophase nuclear morphology; (▲) budding index; (◆) nuclear localization of Pds1; (○) spindle localization of Pds1. (B, a and b) Live cell localization of Pds1GFP. Images of a diploid strain with one endogenous copy of Pds1 fused to GFP (SY202). Scale bar: 10 μm. (C) A strain expressing Pds1GFP and Spc29CFP (SY207) was examined by microscopy using GFP and CFP filter sets. Merged images show colocalization of Pds1 with Spc29 in anaphase (top). Simultaneous staining of Pds1GFP and CFPTub1 is shown at bottom (SY208). (D) The length distribution of spindles visualized by Pds1GFP. Spindles measured on cells treated as described in B.

be derived from its primary amino acid sequence. The NH$_2$-terminal third of the protein retains the ability to interact with Pds1 (not shown). The equivalent region in Cut1, the *S. pombe* homologue, has been shown to interact with Cut2, the functional homologue of Pds1, despite lack of conservation at the primary amino acid level (Kumada et al., 1998). The COOH-terminal region of Esp1 exhibits considerable homology to that of Cut1, *Aspergillus* BimB, and human Esp1 (30–40% identity), and it contains a putative calcium binding site (Fig. 8 A).

To address the importance of the potential calcium binding motif for Esp1 function, we constructed mutants of Esp1, where aspartic acid residues in the site were altered to alanine residues. Deletion of the extreme COOH-terminal region of Esp1, including the putative calcium binding site, rendered the mutant protein incapable of complementing an *esp1^ts* mutation, even when the protein was overexpressed from the *GAL1* promoter (Fig. 8 B). In fact, overexpression at the permissive temperature is lethal in an *esp1^ts* background (data not shown). A mutant protein with a single aspartic acid-to-alanine substitution at position 1568 could rescue an *esp1^ts* mutation when overexpressed from the *GAL1* promoter, whereas a lower dose derived from a low copy plasmid and the endogenous promoter only provided weak suppression of the *esp1^ts* phenotype (Fig. 8 B). A second point mutation introducing the D1570A substitution yielded a mutant Esp1 protein unable to complement growth of an *esp1^ts* mutant even when expressed from the *GAL1* promoter. In fact, overexpression of the D1568A/D1570A protein in the *esp1^ts* background, as in the case of 1-1568 protein, was lethal at the permissive temperature. That the mutant Esp1 proteins exacerbated the *esp1^ts* phenotype but did not alter the growth of wild-type cells (not shown) suggests a weak dominant interfering effect, possibly due to competition for Pds1. These data taken together indicate that the putative calcium binding site in the COOH-terminal region plays a crucial role for Esp1 function.

We set out to characterize the essential function of this site in Esp1 by analyzing the nature of the defects of the
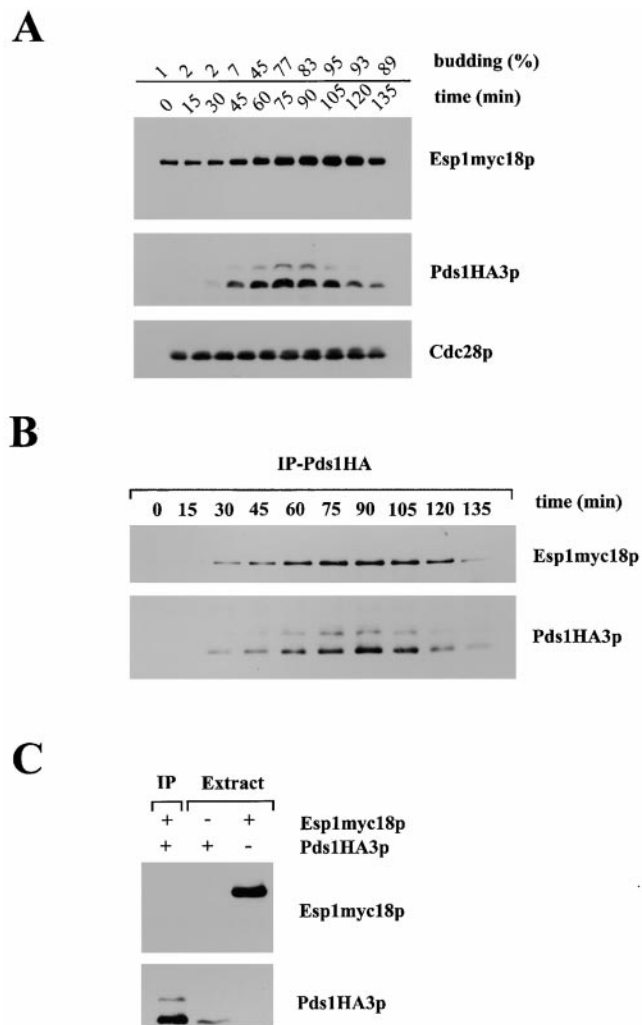
**A**



**B**

IP-Pds1HA

**C**

*Figure 7.* Complex formation between Esp1 and Pds1. (A) A strain expressing endogenous myc18-tagged Esp1 and HA3-tagged Pds1 (SY109) was arrested in G1 by α-factor. After release into YEPDextrose at 22°C, samples were removed at the indicated time points. Extract was analyzed by SDS-PAGE and immunostaining with anti–myc antibody (top), anti–HA antibody (middle), and anti–PSTAIRE antibody, the latter to visualize Cdc28 protein, which serves as a loading control. (B) Extracts prepared from samples in A were subjected to immunoprecipitation using anti–HA antibody to pull down Pds1 protein. SDS-PAGE and immunostaining was carried out with anti–myc antibody to reveal the presence of Esp1 in the precipitate (top) and anti–HA antibody to show amount of precipitated Pds1 (bottom). (C) Esp1/Pds1 complex is not formed in vitro. Extract from a strain expressing Esp1myc18 protein was mixed with extract containing Pds1HA3 protein. After immunoprecipitation with anti–HA antibody and SDS-PAGE, samples were analyzed by immunostaining using anti–myc antibody (top) and anti–HA antibody (bottom).
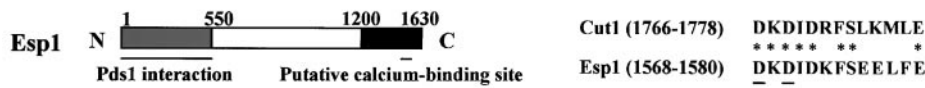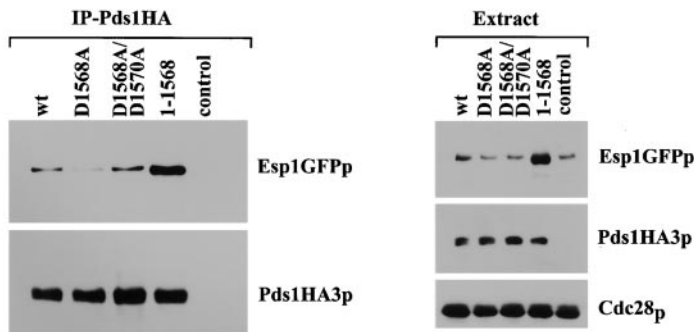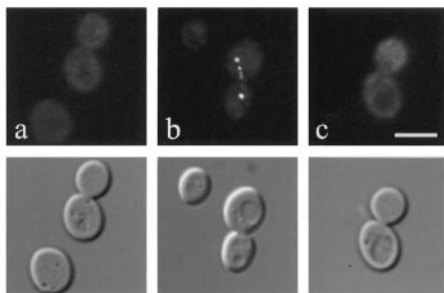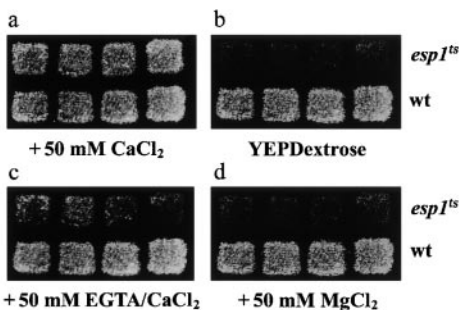
Esp1 mutant proteins. Immunoprecipitation experiments on extracts derived from strains expressing endogenous levels of HA3-tagged Pds1 in combination with the different Esp1GFP mutants induced from the *GAL1* promoter demonstrated that the Esp1 mutants are not defective in Pds1 interaction (Fig. 8 C). The localization of the Esp1 mutant proteins in live cells was subsequently examined

after a brief induction resulting in a comparable 10-fold overexpression in all strains (not shown). The COOH-terminal truncation mutant 1-1568 was delocalized throughout the cell at all stages of the cell cycle, suggesting that the COOH-terminal region of Esp1 is required for nuclear translocation and interaction with the spindle (Fig. 8 D, a). The Esp1 D1568A mutant protein exhibited a distribution similar to wild-type Esp1 protein (Fig. 8 D, b, and Table II), consistent with the fact that overexpression of the mutant from the *GAL1* promoter rescues an *esp1^{ts}* mutation. However, the Esp1 protein carrying two aspartic acid-to-alanine substitutions (D1568A/D1570A) had a severely reduced ability to bind the spindle (Fig. 8 D, c, and Table II). Of >400 large-budded cells examined, only 1.5% displayed spindle labeling, compared with 28.8% in wild-type cells. In addition, no spindles were observed exceeding 4 μm in length. The reduction in spindle association may account for the loss of complementation ability of this double mutant protein. Thus, the putative calcium binding site in the conserved COOH-terminal domain of Esp1 appears to be required to initiate and/or maintain spindle association. When we tested for a possible effect of calcium on Esp1 function, we noticed that addition of extra $CaCl_2$ to the growth medium rescued the temperature sensitivity of *esp1^{ts}* mutants. This suppression could not be achieved by other divalent cations, but was specific to $Ca^{2+}$ and reversible by the addition of the calcium chelator EGTA to the medium (Fig. 8 E). It is therefore possible that calcium may regulate the activity of Esp1, perhaps by promoting spindle association at anaphase.

## Discussion

### A Novel Role of Esp1 in Anaphase Spindle Elongation

Esp1 is a key player in sister chromatid separation. Its liberation from Pds1 mediated by APC-dependent proteolysis is essential to remove cohesion between duplicated sister chromatids, allowing them to separate when microtubule-dependent forces are exerted by the spindle. To date, it has been unclear whether the Esp1/Pds1 complex also regulates aspects of anaphase spindle elongation. Here we report for the first time that a member of the separin family is directly required for spindle elongation at anaphase. In the absence of cohesion, Esp1 activity is still required for anaphase spindle movement. The spindle function of Esp1 is consistent with its cell cycle–dependent localization, reported in this paper. Esp1 has previously been shown to bind the spindle apparatus by indirect immunofluorescence, but in this study only a fraction of the protein was reported to interact with the spindle (Ciosk et al., 1998). By monitoring the localization of Esp1 fused to GFP in real time studies, we found that the majority of Esp1 protein associates with the SPBs and the spindle as cells progress from metaphase to anaphase (Figs. 1 and 2). In G2, Esp1 briefly accumulates in the nucleus before spindle binding. It is therefore tempting to speculate that Esp1 first associates transiently with chromatin to mediate sister chromatid separation, after which it serves as an anaphase signal transducer, translocating to the spindle. A significant pool of Esp1 is located at the spindle midzone during anaphase. This central region of the spindle, where

*Figure 8.* The role of the putative calcium-binding site in the conserved COOH-terminal domain of Esp1. (A) A schematic representation of the domain structure of Esp1. The $NH_2$-terminal domain constituting 1/3 of the protein is sufficient to interact with Pds1. The conserved COOH-terminal region contains a putative calcium binding site, which is conserved in the *S. pombe* homologue Cut1. (B) Complementation ability of various Esp1 mutant proteins in an *esp1$^{ts}$* strain. Proteins were either expressed from an integrated allele driven by the *GAL1* promoter (*GAL1*) or expressed from their own promoter on a low copy plasmid (*ARS/CEN*). The Esp1 mutants were tested for complementation in *esp1$^{ts}$* strain (SY122) with or without the GFP tag with similar results. (C) Mutation in the COOH-terminal region of Esp1 does not affect the ability to interact with Pds1. A strain expressing HA3-tagged Pds1 (SY111) was transformed with integrating plasmids encoding the different Esp1GFP mutant proteins inducible from the *GAL1* promoter. The resulting strains were grown in YEPRaffinose, induced for 80 min with 2% galactose, and extract prepared for immunoprecipitation with anti–HA antibody to bring down Pds1. After SDS-PAGE immunostaining was performed with anti–GFP antibody to visualize Esp1GFP in the precipitate (top) and anti–HA antibody to confirm Pds1 precipitation. (Right) The presence of Esp1GFP, Pds1HA3, and Cdc28 protein in the extract from the different strains is shown. An isogenic strain expressing only Esp1GFP protein (SY104) was included as a control. (D) Localization of mutant Esp1GFP protein in live cells. Strains expressing either *GAL1*-inducible Esp1(1-1568)GFP (SY113), Esp1(D1568A)GFP (SY114), or Esp1(D1568A/D1570A)GFP (SY115) were examined by microscopy after a 20-min induction on solid YEPGalactose media. (a) Esp1(1-1568)GFP, (b) Esp1(D1568A)GFP, and (c) Esp1(D1568A/D1570A)-GFP. (Top) GFP signals; (bottom) DIC. Scale bar: 10 μm. (E) Calcium added to the growth medium can suppress the temperature-sensitive phenotype of *esp1$^{ts}$* mutant. The *esp1-N5* mutant (SY117) and an isogenic wild-type strain grown at room temperature was replica plated onto the following plates: (a) YEPDextrose + 50 mM $CaCl_2$, (b) YEPDextrose, (c) YEPDextrose + 50 mM EGTA/$CaCl_2$, (d) YEPDextrose + 50 mM $MgCl_2$. All plates were incubated for 1 d at 2°C above the restrictive temperature of the *esp1-N5* mutation (37°C). The ability of calcium to suppress the lethality of an *esp1$^{ts}$* mutation was confirmed in several different *esp1$^{ts}$* alleles.

polar microtubules overlap, plays an important role in elongation of the anaphase spindle (Pellman et al., 1995; Winey et al., 1995). Although there is still controversy as to whether anaphase elongation occurs by a pushing or pulling mechanism, studies suggest that in *S. cerevisiae* the nuclear microtubules generate the forces for anaphase spindle elongation (Sullivan and Huffaker, 1992). A recent study of spindle dynamics reveals that elongation of the anaphase spindle in yeast is coupled to microtubule growth at the overlapping plus ends of the spindle midzone (Maddox et al., 2000). The midzone usually becomes highly organized during anaphase, with microtubules from one pole lying adjacent to those from the opposite pole. Electron microscopy studies have revealed that the midzone in *esp1$^{ts}$* mutants lacks organization of the antiparallel microtubules (McGrew et al., 1992). Although this could be an indirect result of the inability of *esp1$^{ts}$* mutants to separate sister chromatids, in the light of our data, it

*Table II. The Distribution of Mutant Esp1GFP Proteins in Live Cells Compared with Wild-Type Esp1GFP*

|  | % | % | % |
|---|---|---|---|
| wt Esp1GFP | 11.6 | 28.8 | 59.6 |
| Esp1(D1568A)GFP | 10.0 | 21.0 | 69.0 |
| Esp1(D1568A/D1570A) GFP | 5.3 | 1.5 | 93.2 |

Cells derived from the strains described in Fig. 8 D were analyzed for Esp1GFP localization. For each strain, >400 cells were counted and placed in the following categories: nuclear localization, spindle localization, or no/dispersed fluorescent signal. The experiment was repeated at least three times with similar results.

more likely reflects a direct role for Esp1 in maintaining proper interdigitation of pole-to-pole microtubules that drive spindle elongation. The midzone association of Esp1 presumably reflects essential aspects of the Esp1 spindle role. It is likely that adequate, but undetectable, amounts of spindle-bound Esp1 remains in *ase1Δ* and *pds1* mutants, which have impaired Esp1 spindle localization (Fig. 3), explaining why these mutants are still viable under unperturbed conditions. Deletion of *ASE1* in an *esp1ts* mutant enhances the temperature sensitivity of the strain, supporting the idea that the midzone is important for Esp1 function. A similar genetic interaction was identified between *tub3Δ* and *esp1ts* mutations (not shown), which further links Esp1 to spindle function.

Whether the Esp1 function at the spindle involves degradation of an unidentified midzone component, regulation of an anaphase motor protein, microtubule polymerization, or a structural role in the organization of microtubules from opposite poles remains unknown. The Esp1 protein itself does not show significant homology to any known motor protein, and it does not interact directly with the known midzone protein Ase1. Identification of potential components of the midzone that interact with Esp1 will provide valuable clues to the exact mechanism of action of Esp1 and how the midzone functions during anaphase spindle elongation in general.

### Pds1 Localization Reflects a Regulatory Role of the Esp1/Pds1 Complex during Anaphase

Pds1 has previously been shown to be a nuclear protein from the time it is produced after bud emergence until it is turned over at the onset of anaphase (Yamamoto et al., 1996). We report the novel finding that Pds1 associates with the spindle apparatus at the metaphase–anaphase transition and that a fraction of Pds1 persists at the SPBs and the spindle midzone into midanaphase. Pds1 may, therefore, like Esp1, be involved in regulating aspects of early anaphase spindle function. The surprising observation that a pool of Pds1 escapes destruction at anaphase onset raises the intriguing question whether distinct subpopulations of Pds1, with specialized tasks, exist in the cell. This would be consistent with the recent report that Pds1, besides its regulatory role at anaphase, also regulates exit of mitosis by preventing release of Cdc14 from the nucleo-

lus, and thus inhibiting cyclin degradation (Cohen-Fix and Koshland, 1999; Shiramaya et al., 1999; Tinker-Kulberg and Morgan, 1999). To this end, it is possible that the remaining pool of Pds1 may be involved in coupling exit of mitosis with the earlier completion of anaphase, either in conjunction with or independently of Esp1. In fact, several components of the mitotic exit network that govern exit of mitosis exhibit SPB localization (Bardin et al., 2000; Song et al., 2000). The reason why a subset of Pds1 resists early degradation is not clear, but may reflect modification or interaction with specific components that delay recognition by the proteolysis machinery.

### Pds1 Targets Esp1 to the Nucleus and Mitotic Spindle

The general view of Pds1 is that it functions as an inhibitor of Esp1 activity. However, the current model does not explain the observations that Esp1 in high dosage can suppress a *pds1ts* mutation or that *esp1ts* and *pds1ts* mutations exhibit synthetic lethality (D.J. Clarke and S.I. Reed, unpublished data), which argue that the two components have overlapping functions in addition to their antagonistic ones. In this study, we present evidence that Pds1 also promotes Esp1 function by ensuring efficient localization of the latter to the nucleus and the spindle, providing an explanation for this apparent paradox. Esp1 only accumulated in the nucleus and associated with the spindle in the presence of functional Pds1 (Figs. 4, b and c, and 5). It is possible that earlier association with Pds1 is needed merely to induce a conformational change in the structure of Esp1 to render it more competent to interact with the spindle. An alternative, and perhaps more plausible, explanation in the light of our data is that Pds1 is directly involved in mediating Esp1 spindle interaction. Thus, there exists a dual-step requirement for Pds1: first, to transport Esp1 into the nucleus and, second, to presumably load it onto the early mitotic spindle. A loading function of Pds1 is consistent with the observation that Pds1 itself interacts with the spindle with similar timing as Esp1, and the relatively brief kinetics of interaction manifest in the shorter spindle length distribution of Pds1-labeled spindles, as compared with Esp1-decorated spindles.

Although Pds1 is required to accumulate Esp1 in the nucleus, Esp1 is not ostensibly excluded from this compartment when Pds1 is absent, either in wild-type G1 or *pds1Δ* cells. This, albeit reduced, activity of Esp1 in the nucleus may indeed explain why deletion of *PDS1* is not lethal at low temperatures.

Pds1 may not be the sole factor that regulates Esp1 localization. In cells expressing Esp1GFPNLS, we saw no significant difference in the timing of nuclear and spindle association of Esp1 as compared with cells expressing Esp1GFP alone. There are several possibilities that could account for this unexpected result. First, the NLS may only become exposed after a structural change in Esp1 as a result of modification induced by an unknown event in late G2. Second, a nuclear export mechanism may operate early in the cell cycle, in the absence of Pds1, to reduce the nuclear amount of Esp1, although the Esp1 protein sequence does not reveal obvious nuclear export signals. Alternatively, and perhaps more likely, a cytoplasmic component may retain most Esp1 protein in the cytoplasm in the early stages of the cell cycle. Studies on the Esp1 homologue in *S. pombe*, Cut1, have hinted at the existence of

such a cytoplasmic retention factor, although its identity remains unknown (Kumada et al., 1998). The presence of such a regulatory factor could also explain the temporal lag between Esp1 and Pds1 nuclear localization. Early work has shown that Pds1 is mostly nuclear at S phase (Yamamoto et al., 1996), whereas we have demonstrated both in live cells and by indirect immunofluorescence that Esp1 first concentrates in the nucleus in late G2. Yet we know that Esp1 and Pds1 form a complex as soon as Pds1 protein appears in the cell cycle. Therefore, the complex must be retained in the cytoplasm until late G2 unless the amount of complex formed early in the cell cycle is below the detection limit of our readout, which cannot be entirely excluded. If a cytoplasmic retention factor exists, it must be limiting as overexpression of Pds1Δdb protein from the *GAL1* promoter allows nuclear accumulation of Esp1 in unbudded cells (Fig. 5 B).

Our data favor a model in which Pds1, through physical interaction, carries Esp1 into the nucleus and positions it efficiently on the spindle at the onset of anaphase. Pds1 presumably has a docking site on the spindle independent of Esp1, as Pds1 spindle localization is unperturbed in *esp1ts* mutants. The Esp1/Pds1 complex binds both SPBs and the early anaphase spindle. What event actually triggers the spindle association is not clear at present, but it may require APC activity and initial degradation of Pds1 (Ciosk et al., 1998; our unpublished observations). Upon Pds1 proteolysis, Esp1 is activated to promote sister chromatid separation, and then presumably in conjunction with remaining Pds1 is translocated to the spindle to mediate anaphase elongation, perhaps through interaction with components of the spindle midzone. This model is consistent with the observation that Esp1 can promote loss of cohesion in the absence of functional kinetochores or mitotic spindles (Ciosk et al., 1998). If Pds1 is indeed directly mediating Esp1 spindle interaction, Esp1 must be loaded on the spindle when a stoichiometric amount of Pds1 still remains. Initially, there must be an excess of Pds1 in the cell, as extra Esp1 from overproduction is largely being cleared from the cytoplasm into the nucleus in a Pds1-dependent manner (compare Fig. 4, A with B). Esp1 persists on the spindle through an independent docking site after spindle-bound Pds1 is degraded.

### *Function of the Conserved COOH-Terminal Domain in Esp1-related Proteins*

The ability to associate with the spindle apparatus depends on the COOH-terminal region of Esp1 as well as the NH$_2$-terminal third of the protein, which mediates interaction with Pds1. We found, more specifically, that a putative calcium binding site in the COOH terminus of Esp1 is important for proper anaphase spindle function, as an Esp1 mutant with the two amino acid substitutions D1568A/D1579A in this motif had a strongly reduced (~20-fold) spindle binding ability and only labeled spindles shorter than 4 $\mu$m (Table II). Indeed, a single mutation at position 1568 was sufficient to yield a mutant Esp1 protein unable to complement an *esp1ts* mutation. A similar behavior was recently described for Cut1 alleles mutated in the COOH-terminal region (Kumada et al., 1998). In this study, a Cut1 mutant with a single amino acid change at position 1767, which lies within the potential calcium binding motif, was shown to localize to metaphase

spindles but was excluded from anaphase spindles. Thus, the COOH-terminal calcium-binding motif is likely to have equivalent essential roles in Esp1 and Cut1, ensuring proper association of the protein with the spindle during anaphase. It cannot be ruled out that these separin mutants are also defective in triggering loss of cohesion and that the observed effect on spindle binding is indirect.

Whether the conserved calcium binding motif in Esp1 and Cut1 actually mediates calcium binding remains to be shown. Interestingly, *esp1ts* mutations were suppressed by the addition of calcium to the growth medium, which could be reversed by simultaneous addition of the chelating agent EGTA. This, together with our finding that mutations in two genes important for calcium homeostasis are lethal in combination with an *esp1ts* mutation (our unpublished data), raises the intriguing possibility that calcium may regulate Esp1 activity. It has previously been reported that calcium oscillations occur at the metaphase-to-anaphase transition and play an important role in anaphase onset (Groigno and Whitaker, 1998), although this has yet to be established in yeast.

It is not surprising that Esp1 is regulated by several mechanisms given the importance of sister chromatid separation for the survival of the cell. Once cohesion has been established during DNA replication, it becomes pivotal that Esp1 activity is controlled to coordinate loss of cohesion with anaphase spindle elongation. The fact that *pds1Δ* cells do not separate sisters prematurely (Ciosk et al., 1998; D.J. Clarke, unpublished data) clearly indicates that alternative mechanisms exist to regulate Esp1 activity.

The Esp1 and Pds1 complex appears to be conserved in organisms of different origin. Their best characterized homologues in *S. pombe*, Cut1 and Cut2, perform equivalent vital roles in sister chromatid separation. Recently, both Cut1 and Cut2 were found to interact with the spindle, and this association (but not the nuclear localization of Cut1) was dependent on Cut2. Thus, given the overall similarities in the regulation and function of the Esp1/Pds1 and Cut1/Cut2 complexes, it seems reasonable to assume that similar functional relationships exist between homologues of Esp1 and Pds1 in higher eukaryotic cells.

### References

Alexandru, G., W. Zachariae, A. Schleiffer, and K. Nasmyth. 1999. Sister chromatid separation and chromosome re-duplication are regulated by different mechanisms in response to spindle damage. *EMBO (Eur. Mol. Biol. Organ.) J.* 18:2707–2721.

Bardin, A.J., R. Visintin, and A. Amon. 2000. A mechanism for coupling exit of mitosis to partitioning of the nucleus. *Cell.* 102:21–31.

Ciosk, R., W. Zachariae, C. Michaelis, A. Shevchenko, M. Mann, and K. Nasmyth. 1998. An ESP1/PDS1 complex regulates loss of sister chromatid

cohesion at the metaphase to anaphase transition in yeast. *Cell*. 93:1067–1076.

Clarke, D.J., M. Segal, G. Mondesert, and S.I. Reed. 1999. The Pds1 anaphase inhibitor and Mec1 kinase define distinct checkpoints coupling S phase with mitosis in budding yeast. *Curr. Biol*. 9:365–368.

Cohen-Fix, O., and D. Koshland. 1999. Pds1p of budding yeast has dual roles: inhibition of anaphase initiation and regulation of mitotic exit. *Genes Dev*. 13:1950–1959.

Cohen-Fix, O., J.-M. Peters, M.W. Kirschner, and D. Koshland. 1996. Anaphase initiation in *Saccharomyces cerevisiae* is controlled by the APC-dependent degradation of the anaphase inhibitor Pds1p. *Genes Dev*. 10:3081–3093.

Funabiki, H., K. Kumada, and M. Yanagida. 1996. Fission yeast Cut1 and Cut2 are essential for sister chromatid separation, concentrate along the metaphase spindle and form large complexes. *EMBO (Eur. Mol. Biol. Organ.) J*. 15:6617–6628.

Goh, P.Y., and J.V. Kilmartin. 1993. NDC10: a gene involved in chromosome segregation in *Saccharomyces cerevisiae*. *J. Cell Biol*. 121:503–512.

Groigno, L., and M. Whitaker. 1998. An anaphase calcium signal controls chromosome disjunction in early sea urchin embryos. *Cell*. 92:193–204.

Guthrie, C., and G.R. Fink. 1991. Guide to yeast genetics and molecular biology. Vol. 194. Academic Press, Inc., San Diego, CA.

Juang, Y.-L., J. Huang, J.-C. Peters, M.E. McLaughlin, C.-Y. Tai, and D. Pellman. 1997. APC-mediated proteolysis of Ase1 and the morphogenesis of the mitotic spindle. *Science*. 275:1311–1314.

Kaiser, P., V. Moncollin, D.J. Clarke, M.H. Watson, B.L. Bertolaet, S.I. Reed, and E. Bailly. 1999. Cyclin-dependent kinase and Cks/Suc1 interact with the proteosome in yeast to control proteolysis of M-phase targets. *Genes Dev*. 13:1190–1202.

Kumada, K., T. Nakamura, K. Nagao, H. Funabiki, T. Nakagawa and M. Yanagida. 1998. Cut1 is loaded onto the spindle by binding to Cut2 and promotes anaphase spindle movement upon Cut2 proteolysis. *Curr. Biol*. 8:633–641.

Maddox, P.S., K.S. Bloom, and E.D. Salmon. 2000. The polarity and dynamics of microtubule assembly in the budding yeast *Saccharomyces cerevisiae*. *Nat. Cell Biol*. 2:36–41.

May, G.S., C.A. McGoldrick, C.L. Holt, and S.H. Denison. 1992. The *bimB3* mutation of *Aspergillus nidulans* uncouples DNA replication from the completion of mitosis. *J. Biol. Chem*. 267:15737–15743.

McGrew, J.T., L. Goetsch, B. Byers, and P. Baum. 1992. Requirement for ESP1 in the nuclear division of *Saccharomyces cerevisiae*. *Mol. Biol. Cell*. 3:1443–1454.

Michaelis, C., R. Ciosk, and K. Nasmyth. 1997. Cohesins: chromosomal proteins that prevent premature separation of sister chromatids. *Cell*. 91:35–45.

Mondesert, G., D.J. Clarke, and S.I. Reed. 1997. Identification of genes controlling growth polarity of the budding yeast *Saccharomyces cerevisiae*: a possible role of *N*-glycosylation and involvement of the exocyst complex. *Genetics*. 147:421–434.

Pellman, D., M. Bagget, H. Tu, and G.R. Fink. 1995. Two microtubule-associated proteins required for anaphase spindle movement in *Saccharomyces cerevisiae*. *J. Cell Biol*. 130:1373–1385.

Richardson, H.E., C. Wittenberg, F.R. Cross, and S.I. Reed. 1989. An essential G1 function for cyclin-like proteins in yeast. *Cell*. 59:1127–1133.

Shiramaya, M., A. Toth, M. Galova, and K. Nasmyth. 1999. APC[Cdc20] promotes exit from mitosis by destroying the anaphase inhibitor Pds1 and cyclin Clb5. *Nature*. 11:203–207.

Sikorski, R.S., and P. Hieter. 1989. A system of shuttle vectors and yeast host strains designed for efficient manipulation of DNA in *Saccharomyces cerevisiae*. *Genetics*. 122:19–27.

Song, S., T.Z. Grenfell, S. Garfield, R.L. Erikson, and K.S. Lee. 2000. Essential function of the polo box of Cdc5 in subcellular localization and induction of cytokinetic structures. *Mol. Cell. Biol*. 20:286–298.

Straight, A.F., W.F. Marshall, J.W. Sedat, and A.W. Murray. 1997. Mitosis in living budding yeast: anaphase A but no metaphase plate. *Science*. 277:574–578.

Sullivan, D.S., and T.C. Huffaker. 1992. Astral microtubules are not required for anaphase B in *Saccharomyces cerevisiae*. *J. Cell Biol*. 119:379–388.

Tang, Y., and S.I. Reed. 1993. The Cdk-associated protein Cks1 functions both in G1 and G2 in *Saccharomyces cerevisiae*. *Genes Dev*. 7:822–832.

Tinker-Kulberg, R.L., and D.O. Morgan. 1999. Pds1 and Esp1 control both anaphase and mitotic exit in normal cells and after DNA damage. *Genes Dev*. 13:1936–1949.

Uhlmann, F., F. Lottspeich and K. Nasmyth. 1999. Sister-chromatid separation at anaphase onset is promoted by cleavage of the cohesin subunit Scc1. *Nature*. 400:37–42.

Uzawa, S., I. Sameijima, T. Hirano, K. Tanaka, and M. Yanagida. 1990. The fission yeast cut1[+] gene regulates spindle pole body duplication and has homology to the budding yeast ESP1 gene. *Cell*. 62:913–925.

Wach, A., A. Brachat, R. Pohlmann, and P. Philippsen. 1994. New heterologous modules for classical or PCR-based gene disruptions in *Saccharomyces cerevisiae*. *Yeast*. 10:1793–1808.

Winey, M., C.L. Mamay, E.T. O'Toole, D.N. Mastronarde, T.H. Giddings, K.L. McDonald, and J.R. McIntosh. 1995. Three-dimensional ultrastructural analysis of the *Saccharomyces cerevisiae* mitotic spindle. *J. Cell Biol*. 129:1601–1615.

Yamamoto, A., V. Guacci, and D. Koshland. 1996. Pds1p is required for faithful execution of anaphase in the yeast, *Saccharomyces cerevisiae*. *J. Cell Biol*. 133:85–97.

Zachariae, W., and K. Nasmyth. 1996. TPR proteins required for anaphase progression mediate ubiquitination of mitotic B-type cyclins in yeast. *Mol. Biol. Cell*. 7:791–801.

Zou, H., T.J. McGarry, T. Bernal, M.W. Kirschner. 1999. Identification of a vertebrate sister-chromatid separation inhibitor involved in transformation and tumorigenesis. *Science*. 285:418–422.